(for X^-) or staircase (for HgX_3^-) voltammetry using the same electrode (SMDE, dropping mode) and solutions, and using a conventional DME. The third columns in Tables IV and V contain values calculated from data included in the previous paper[1] and data which will be described elsewhere.[2] Since the normal pulse reduction wave of HgX_3^- does not have a well-developed limiting plateau (rather a maximum caused by slow processes associated with the reduction of adsorbed species), we had to utilize staircase voltammetry as the reference method for determination of D for the HgX_3^- ions. Except for the value of D for iodide ions obtained from the polarographic data (DME) and the value of D for triiodomercurate ions from the chronocoulometric data, all results are in good agreement. Notice that the changes of D within the halide ions and within the trihalomercurate ions are opposite to those which might be expected from the dimensions of the ions. The smallest halide ion, Cl^-, and the smallest trihalomercurate ion, $HgCl_3^-$, have the smallest diffusion coefficients. A reasonable explanation is that the smaller ions, having a larger charge density, are more efficiently solvated by polar molecules of the solvent.

The diffusion coefficient of iodide ions in acetonitrile was determined by Macagano et al.[18] using a platinum rotating disk electrode and by DePauli et al.[19] by means of chronopotentiometry. In both cases high concentrations of iodide (8–18 mM) were used and the supporting electrolyte contained Li^+ and Na^+ ions. In the previous paper[1] we reported evidence for the existence of Li^+Cl^- ion pairs in acetonitrile. The formation of ion pairs between I^- and Li^+ or Na^+ might be responsible for lower (1.68×10^{-5} cm^2 s^{-1} (ref 18)) values of D obtained in solutions containing lithium or sodium salts.

Registry No. $HgCl_3^-$, 14988-07-9; $HgBr_3^-$, 21388-05-6; HgI_3^-, 19964-11-5; Cl^-, 16887-00-6; Br^-, 24959-67-9; I^-, 20461-54-5; Hg, 7439-97-6.

(18) Macagano, V. A.; Giordano, M. C.; Arvia, A. J. *Electrochim. Acta* **1969**, *14*, 335–57.
(19) DePauli, C.; Iwasita, T.; Giordano, M. C. *J. Electroanal. Chem.* **1973**, *45*, 233–45.
(20) Coetzee, J. F.; Campion, J. J.; Liberman, D. R. *Anal. Chem.* **1973**, *45*, 343–7.
(21) "Handbook of Chemistry and Physics", 61st ed.; CRC Press: Boca Raton, FL, 1980.

Effect of Chain Length on Mesomorphism of Steroid Esters of 4-(4-Alkylphenyl-X)benzoic Acids with X = CO, O, S, and CH_2

Mitsuhiro Koden, Tadao Yagyu, Shunsuke Takenaka,* and Shigekazu Kusabayashi

Department of Applied Chemistry, Faculty of Engineering, Osaka University, Suita, Osaka 565, Japan *(Received: October 20, 1982; In Final Form: March 8, 1983)*

To examine the effect of bent shapes on mesomorphic properties a homologous series of steroid esters have been prepared: $H(CH_2)_n$-4-C_6H_4-X-4-C_6H_4COOR, X = CO, O, S, CH_2, R = cholesteryl, β-sitosteryl, cholestanyl, stigmasteryl, ergosteryl; n = 0–15. The chain elongation results in an increase in not only the molecular length but also the breadth due to the angular linkage, X. The steroid portions are of primary importance for the mesomorphic properties of the present series, and the thermal stability of the mesophases is strongly dependent on the mesogenic power of the aryl portions, where the effective order is CO > O > S > CH_2. The transition enthalpies and entropies for the smectic A–cholesteric and cholesteric–isotropic (Ch–I) transitions are almost independent of the chain length of the alkyl group, indicating that a long alkyl chain has no role from a thermodynamical point of view. Within the mesophases, the aryl and steroid cores are assumed to be piled up, interacting with each other, and the alkyl groups are apart from each other to avoid short-range interaction.

Introduction

It has been known that linearity, rigidity, and polarity are indispensable for displaying thermotropic liquid crystallinity.[1] Many mesogenic molecules hitherto reported have a hard-core portion consisting of aromatic rings and a relatively flexible terminal portion of alkyl chains

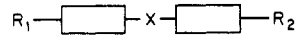

where the central linkage, X, is usually —C=C—, —N=N—, —C=N—, —COO—, and so on. Some groups such as –CO–, –O–, –S–, and $-CH_2-$ reduce the thermal stability of mesomorphic states due to their bent shapes. Therefore, these groups are called nonmesogenic linkages.[2] Recently, we reported that some cholesteryl esters of 4-arylbenzoic acids involving these linkages gave rise to highly stable mesophases, in spite of molecular distortion.[3] Our interest in this paper is the effect of chain elongation on the themal stability of the compounds in Chart I. As can be seen from the structures, the mean axis of the alkyl chain at the aryl ring makes an angle of ca. 60° with respect to the longer axis involving the steroid core, and the chain elongation will lead to an increase in not only the molecular length but also the breadth, simultaneously. The molecular bend around the molecular center is assumed not to favor an anisotropic alignment of molecules. We will report the preparations and the thermal properties of the homologous

(1) G. R. Luckhurst and G. W. Gray, "The Molecular Physics of Liquid Crystals", Academic Press, New York, 1979.
(2) C. Destrade, N. H. Tinh, and H. Gasparoux, *Mol. Cryst. Liq. Cryst.*, **59**, 273 (1980); C. Destrade, F. Vinet, P. Maelstaf, and H. Gasparoux, *ibid.*, **68**, 175 (1981).
(3) M. Koden, S. Takenaka, and S. Kusabayashi, *Mol. Cryst. Liq. Cryst.*, **88**, 137 (1982).

0022-3654/83/2087-4730$01.50/0

Chart I

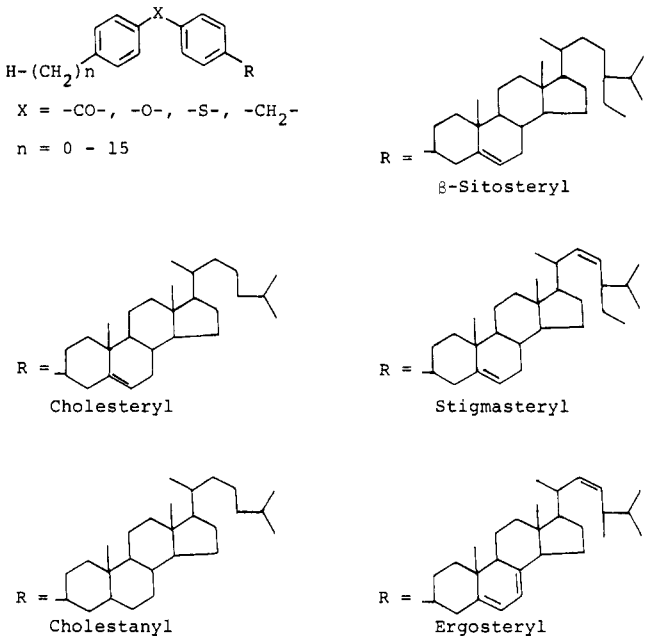

series, and the mesomorphic properties are discussed in electronic and structural terms.

Experimental Section

Melting points and transition temperatures were determined by using a Nikon PM polarizing microscope equipped with a Mettler FP-52 heating stage and control unit. Transition enthalpies were determined by using a Daini-Seikosha differential scanning calorimeter Model SSC-560, where indium (99.9%) was used as a calibration standard with a heating rate of 5 °C, and the entropies were calculated by using the equation, $\Delta S = \Delta H/T$. The X-ray experiments were done by using CuK radiation (λ = 1.54 Å) and a Laue camera modified to study scattering at small angles. The samples used were contained in capillaries (diameter = ca. 1 mm). The specimen was mounted in a copper block whose temperature was controlled within 0.1 °C, and measured with a thermocouple located near the sample.

4-(4-Nonylbenzoyl)benzoic Acid. A solution of *n*-nonylbenzene (0.12 mol) in dry dichloromethane (50 mL) was added dropwise with vigorous stirring to a mixture of terephthaloyl chloride (0.12 mol) and aluminum trichloride (0.24 mol) in dry dichloromethane (300 mL) at room temperature. The mixture was stirred at room temperature for 5 h and then poured onto ice (200 g) and concentrated hydrochloric acid (20 mL), and the organic layer was separated, washed with water, and dried over Na_2SO_4. After removal of solvent, the residue was heated in a mixed solution of sodium hydroxide (0.3 mol) in water (100 mL) and ethanol (50 mL) under reflux for 2 h. When cooled, the mixture was acidified with concentrated hydrochloric acid. The precipitate was filtered off, washed with water, and dried. The product was then purified by means of column chromatography on silica gel, using a solvent mixture of ether and *n*-hexane (5:95–20:80). The eluent was recrystallized from a mixed solvent of benzene–ethanol (1:1–2:1), yielding 4-(4-nonylbenzoyl)benzoic acid as colorless needles: yield 18%, mp 168–169 °C.

4-(4-Nonylphenoxy)benzoic Acid. A solution of *n*-nonanoyl chloride (0.1 mol) in dry dichloromethane (50 mL) was added dropwise with vigorous stirring to a mixture of diphenyl ether (0.1 mol) and aluminum trichloride (0.1 mol) in dry dichloromethane (300 mL) at 0 °C. The mixture was stirred at room temperature for 5 h and then poured onto ice (200 g) and concentrated hydrochloric acid (20 mL); the organic layer was separated, washed with water, and dried over Na_2SO_4. Removal of solvent gave 4-nonanoyldiphenyl ether, which was recrystallized from ethanol. A mixture of 4-nonanoyldiphenyl ether (0.05 mol), aqueous hydrazine (15 mL), and potassium hydroxide (15 g) in triethylene glycol was heated at 150 °C for 1 h.[4] The temperature was gradually raised, and the mixture was heated at 230 °C for 3 h. The resulting solution was then cooled and neutralized with a solution of ice and concentrated hydrochloric acid. The organic fraction was extracted with ether and dried (Na_2SO_4). Removal of the solvent and distillation under vacuum gave a 62% yield of 4-nonyldiphenyl ether (bp 167–171 °C/1 mmHg).

A solution of acetyl chloride (0.03 mol) in dry dichloromethane (25 mL) was added dropwise with vigorous stirring to a mixture of 4-nonyldiphenyl ether (0.03 mol) and aluminum trichloride (0.03 mol) in dry dichloromethane (150 mL) at 0 °C. The mixture was stirred at room temperature for 5 h and then poured onto ice (100 g) and concentrated hydrochloric acid (10 mL), and the layers were separated. The organic layer was washed with water, dried (Na_2SO_4), and evaporated to dryness, giving 4-acetyl-4′-nonyldiphenyl ether. To a solution of bromine (20 g), sodium hydroxide (17 g), and water (70 mL) was added dropwise 4-acetyl-4′-nonyldiphenyl ether (0.015 mol) in ethanol (300 mL) at 0 °C. The mixture was stirred at 40 °C for 3 h. When cooled, the mixture was then acidified with concentrated hydrochloric acid and sodium bisulfite was then added to remove excess hypobromite. The precipitate was filtered, washed with water, and dried. Recrystallization from *n*-hexane gave a 57% yield of 4-(4-nonylphenoxy)benzoic acid (mp 111 °C).

4-(4-Alkylbenzoyl)benzoic acids were prepared by the method used for the preparation of 4-(4-nonylbenzoyl)-benzoic acid.

4-(4-Alkylphenoxy)benzoic acids and 4-[(4-alkylphenyl)thio]benzoic acids were prepared by the method used for the preparation of 4-(4-nonylphenoxy)benzoic acid.

4-(4-Alkylbenzyl)benzoic acids were prepared from 4-(4-alkylbenzoyl)benzoic acids by the method used for the hydrazine reduction of 4-nonanoyldiphenyl ether.

Steroid Esters. Cholesterol, cholestanol, β-sitosterol, stigmasterol, and ergosterol were purchased from Nakarai Chemical Co. and were purified by column chromatography on silica gel using a solvent mixture of ether and *n*-hexane (10:90). The acid chlorides of 4-(4-alkylphenyl-X)benzoic acids were reacted with cholesterol in benzene under the presence of pyridine, giving series I–IV (see Table I), which were purified by column chromatography on silica gel, using a solvent mixture of ether and *n*-hexane (5:95), followed by recrystallization from a mixed solvent of benzene and ethanol (5:95).[5]

Cholestanyl, β-sitosteryl, stigmasteryl, and ergosteryl esters were obtained by a method similar to that mentioned above. The elemental analyses are listed in Table I.

Results

Thermal data for series I are summarized in Table II, and the transition temperatures are plotted against the number of carbon atoms, *n*, in the normal alkyl chain in Figure 1A. The first seven (*n* = 0–6) members exhibit only a cholesteric phase. The cholesteric–isotropic transition

(4) H. Minlon, *J. Am. Chem. Soc.*, 68, 2487 (1946).
(5) G. W. Gray, *J. Chem. Soc.*, 3733 (1956).

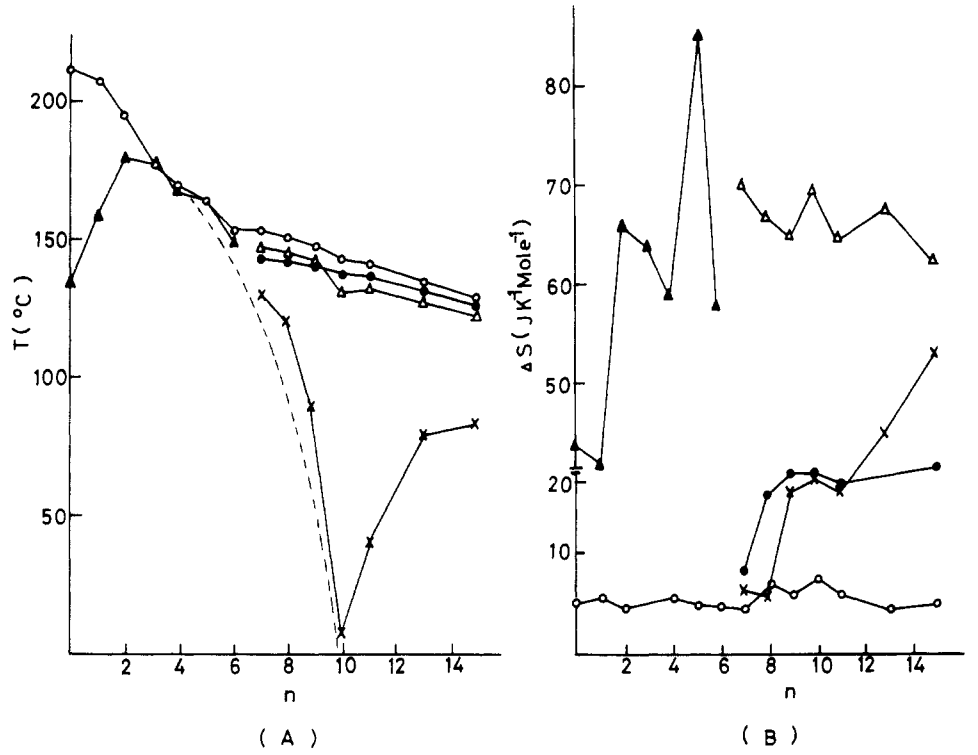

Figure 1. A: Plot of transition temperatures against alkyl chain length (n) for cholesteryl 4-(4-alkylbenzoyl)benzoates (I). B: Plot of transition entropies against chain length (n) for I. O: Cholesteric–isotropic. ●: Smectic A–cholesteric. △: S_2–cholesteric or smectic A. ▲: S_1–cholesteric or isotropic. ×: S_1–S_2.

TABLE I

compd	n	formula	calcd, % C	calcd, % H	found, % C	found, % H
I	0	$C_{41}H_{54}O_3$	82.78	9.15	82.67	9.14
I	1	$C_{42}H_{56}O_3$	82.85	9.27	82.75	9.34
I	2	$C_{43}H_{58}O_3$	82.91	9.38	82.83	9.49
I	3	$C_{44}H_{60}O_3$	82.97	9.49	82.72	9.64
I	4	$C_{45}H_{62}O_3$	82.03	9.60	82.80	9.62
I	5	$C_{46}H_{64}O_3$	83.08	9.70	82.90	9.74
I	6	$C_{47}H_{66}O_3$	83.13	9.80	82.88	9.88
I	7	$C_{48}H_{68}O_3$	83.13	9.89	83.25	9.80
I	8	$C_{49}H_{70}O_3$	83.23	9.98	83.12	10.06
I	9	$C_{50}H_{72}O_3$	83.28	10.06	83.16	10.09
I	10	$C_{51}H_{74}O_3$	83.32	10.15	83.57	10.01
I	11	$C_{52}H_{76}O_3$	83.36	10.23	83.26	10.21
I	13	$C_{54}H_{80}O_3$	83.45	10.38	83.43	10.36
I	15	$C_{56}H_{84}O_3$	83.52	10.52	83.36	10.53
II	0	$C_{40}H_{54}O_3$	82.43	9.34	82.22	9.39
II	6	$C_{46}H_{66}O_3$	82.83	9.97	82.69	9.93
II	9	$C_{49}H_{72}O_3$	83.00	10.23	82.81	10.25
II	10	$C_{50}H_{74}O_3$	83.05	10.31	82.89	10.38
II	11	$C_{51}H_{76}O_3$	83.10	10.39	82.86	10.48
III	0	$C_{40}H_{54}O_2S$	80.22	9.09	80.10	9.10
III	9	$C_{49}H_{72}O_2S$	81.16	10.01	80.99	10.07
III	10	$C_{50}H_{74}O_2S$	81.24	10.10	81.07	10.24
III	11	$C_{51}H_{76}O_2S$	81.33	10.17	81.20	10.19
IV	0	$C_{41}H_{56}O_2$	84.77	9.72	84.95	9.87
IV	10	$C_{51}H_{76}O_2$	84.82	10.75	84.64	10.68
IV	11	$C_{52}H_{78}O_2$	84.84	10.82	84.63	10.60
cholestanyl		$C_{52}H_{78}O_3$	83.10	10.39	83.28	10.46
β-sitosteryl		$C_{54}H_{80}O_3$	83.41	10.30	83.21	10.54
stigmasteryl		$C_{54}H_{76}O_3$	83.63	10.06	83.45	9.97
ergosteryl		$C_{53}H_{74}O_3$	83.82	9.74	83.65	9.58

temperature (T_{Ch-I}) is seen in Figure 1A to monotonically decline on going along the series, without exhibiting the usual even–odd effect. Smectic properties are first encountered for the heptyl homologue and are permitted up to the last homologue under study. The smectic phase shows a homeotropic alignment in between two glasses. Unlike the usual smectic phase, the gradual lowering of thermal stability of the smectic phase on moving along the series is shown in Figure 1A. In addition, all esters past the heptyl homologue have two stable states, namely, S_1 and S_2, which will be assigned to the crystalline states in the later portion. The S_1–S_2 transition temperature descends steeply (n = 7–10), giving a minimum at n = 10, and ascends steeply thereafter.

The entropy changes for the transitions are plotted against n in Figure 1B. The entropy for the cholesteric–isotropic transition is almost constant throughout the series. Thereby, the averaged value is 1.0 J K^{-1} mol^{-1}. The entropy for the smectic A–cholesteric transition stays constant from the octyl to the pentadecyl homologue, where the averaged value is 3.6 J K^{-1} mol^{-1}. Although the entropy for the S_2–cholesteric or –smectic A transition is relatively large, it also stays constant, rather showing a decreasing trend with increasing n. On the other hand, the transition entropy for the solid S_1–S_2 transition shows an increasing trend monotonically with increasing n.

To identify these mesophases, the binary phase diagrams were examined. In Figure 2A, the isobaric diagram for a mixture of the C_{11} homologue of I and cholesteryl myristate which forms the cholesteric and smectic A phases is shown. The miscibility relation indicates that the smectic phase for the C_{11} homologue of I is a smectic A modification. The mixture shows a eutectic phenomenon at 62 °C, suggesting that the S_2 phase is a crystalline phase. The line for the smectic A to cholesteric phase transitions shows a nonlinear relation, and the deviation becomes notable with increasing concentration of the C_{11} homologue of I. In Figure 2B is shown the binary phase diagram for a mixture of the C_{11} homologue of I and cholesteryl benzoate. Two facts worthy of note are that the mixture shows a double eutectic behavior at 110 and 113 °C, and the cholesteric–isotropic transition temperature slightly deviates from ideality. In Figure 2C, on the other hand, the diagram for binary mixtures of the C_{11} and C_0 homologues of I appears quite normal, where the mixture shows a eutectic point at

TABLE II: Transition Temperatures, Enthalpies, and Entropies of Cholesteryl 4-(4-Alkylbenzoyl)benzoates[a]

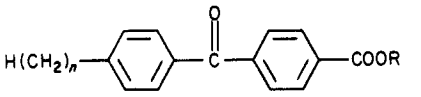

	S_1-S_2, Ch, or I			S_2-S_A or Ch			S_A-Ch			Ch-I		
n	T	ΔH	ΔS	T	ΔH	ΔS	T	ΔH	ΔS	T	ΔH	ΔS
0	134.2	17.9	44.0							210.3	0.50	1.0
1	158.3	17.9	41.4							205.9	0.54	1.0
2	179.0	29.9	66.0							193.1	0.42	0.9
3	174.3	28.5	63.6							(169.2	-	-)
4	167.3	26.0	58.9							169.5	0.50	1.1
5	162.5	39.3	90.2							162.5	0.42	1.1
6	151.3	24.6	57.6							153.1	0.38	0.9
7	129.4	2.4	6.0	148.1	29.6	70.3	(142.6	0.67	1.6)	152.8	0.38	0.9
8	120.9	2.2	5.6	144.4	27.9	66.9	(142.6	1.34	3.2)	149.8	0.59	1.4
9	89.1	5.9	16.4	139.9	26.9	65.1	139.9	1.47	3.6	147.1	0.50	1.2
10	6.6	5.5	17.9	130.0	28.8	69.4	135.7	1.47	3.6	142.0	0.63	1.5
11	40.8	5.1	16.2	132.8	26.2	64.5	135.9	1.38	3.4	141.4	0.50	1.2
13	77.9	7.7	21.9	127.9	27.1	67.6	132.0			133.8	0.38	0.9
15	82.3	10.8	30.3	123.7	24.7	62.2	124.1	1.51	3.8	127.3	0.38	1.0

[a] R = cholesteryl. T: transition temperature (°C). ΔH: transition enthalpy (kJ mol^{-1}). ΔS: transition entropy (J K^{-1} mol^{-1}). (): monotropic transition.

TABLE III: Transition Temperatures, Enthalpies, and Entropies of

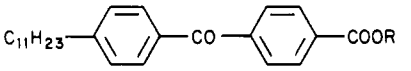

R	T_{MP}, °C	ΔH_{MP}, kJ mol^{-1}	ΔS_{MP}, J K^{-1} mol^{-1}	T_{Ch-I},[a] °C	ΔH_{Ch-I}, kJ mol^{-1}	ΔS_{Ch-I}, J K^{-1} mol^{-1}
cholesteryl	130.0	27.95	65.27	142.0	0.63	1.55
cholestanyl	131.5	28.95	71.54	(128.8)		
β-sitosteryl	131.5	27.85	68.82	(122.3)[b]		
stigmasteryl	126.6	33.69	84.29	(116.2)[b]	2.38	6.12
ergosteryl	129.3	39.61	98.42			

[a] Parentheses indicate monotropic transition. [b] Smectic-isotropic transition.

TABLE IV: Transition Temperatures and Entropies of II, III, and IV[a]

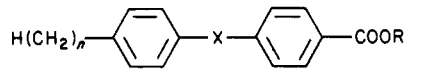

		C-S_A, Ch, I		S_A-Ch		Ch-I	
n	X	T, °C	ΔS, J K^{-1} mol^{-1}	T, °C	ΔS, J K^{-1} mol^{-1}	T, °C	ΔS, J K^{-1} mol^{-1}
0	O	154.3	71.8			176.5	0.65
6	O	145.6	80.2	(103.0)	0.52	145.6	1.04
9	O	126.9	99.8	(96.5)	0.36	130.5	1.05
10	O	124.4	121.3	(99.3)	0.56	124.4	1.24
0	S	135.7	72.3			(91.5)	0.50
9	S	99.4	114.9				
10	S	91.4	147.9			[45]	
11	S	92.3	59.6			[35]	
0	CH_2	173.8	82.3			[100]	
10	CH_2	107.2	18.0[b]				
11	CH_2	105.6	25.8[c]			[50]	

[a] X = O (II), S (III), and CH_2 (IV); R = cholesteryl. Parentheses and brackets indicate monotropic and virtual transition temperatures, respectively. [b] This compound experienced crystal-crystal transition at 92.3 °C. [c] This compound experienced crystal-crystal transition at 95.5 °C.

90 °C and the cholesteric–isotropic transition temperature gives a straight line.

Table III indicates the thermal properties for the steroid esters of 4-(4-undecylbenzoyl)benzoic acid. Although these have similar melting points, their mesomorphic properties are slightly different. The esters of cholesterol and cholestanol give rise to the cholesteric phase, whereas the esters of β-sitosterol and stigmasterol show only smectic properties. On the other hand, the ergosteryl ester is nonmesogenic. These characteristic features are very similar to those for the respective alkanoates.

Thermal properties for cholesteryl esters having diphenyl ether (II), diphenyl thioether (III), and diphenylmethane (IV) cores are summarized in Table IV. Although Table IV indicates only the highest melting point for the homologous series, some of them have plural metastable crystalline phases and show polymelting behaviors. The polymorphism in connection with their bent shapes will be published elsewhere. The cholesteric phase is observed in the homologous series of II and the C_0 ho-

TABLE V

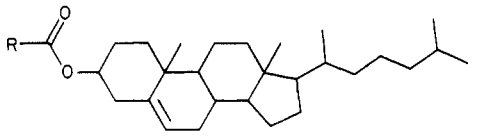

R		transition temp,[a] °C $n = 0$	transition temp,[a] °C $n = 11$	commencement of smectic phase
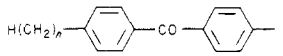	I	210.3	142.0[b]	C-7
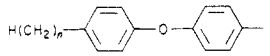	II	176.5	127.7[c]	
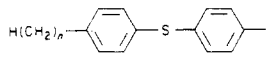	III	(92)	[36]	
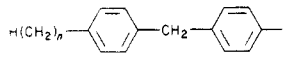	IV	[100]	[60]	
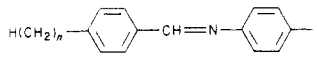	V	(350)[d]	(301)[e]	C-7
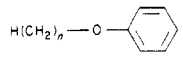	VI	180	209[f]	C-7
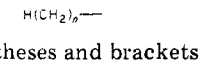	VII	(60.5)	(90)[g]	C-6

[a] Parentheses and brackets indicate monotropic and virtual transition temperatures, respectively. [b] $T_{S_A\text{-Ch}} = 135.9$ °C. [c] $T_{S_A\text{-Ch}} = 99.4$ °C. [d] Unpublished result in our laboratory. [e] $T_{S_A\text{-Ch}} = 225$ °C (J. S. Dave and G. Kurian, *Mol. Cryst. Liq. Cryst.*, 24, 347 (1974)). [f] $T_{S_A\text{-Ch}} = 177.5$ °C (J. S. Dave and R. A. Vora, "Liquid Crystals and Ordered Fluids", Plenum Press, New York, 1970, p 477). [g] $T_{S_A\text{-Ch}} = 81.9$ °C (ref 5).

mologue of III, and the smectic A phase is observed only in the homologous series of II. For series II, the thermal properties are quite similar to those for series I. That is, the entropies for the cholesteric–isotropic and smectic A–cholesteric transitions are likely to be almost independent of the chain length. The homologous series of III and IV are nonmesogenic, except cholesteryl 4-phenylthiobenzoate. The virtual cholesteric–isotropic transition temperatures were obtained from an examination of the binary phase diagram. Figure 2D, for example, indicates a binary phase diagram for a mixture of the C_{11} homologue of III, which has a melting point of 92.3 °C, and cholesteryl 4-benzoylbenzoate. The cholesteric–isotropic transition temperature shows a negative deviation from a straight line, where the virtual transition temperature was extrapolated to be 35 °C.

Thus, the efficiency order for the thermal stability of the cholesteric phase is CO > O > S > CH_2 in both C_0 and C_{11} homologues.

Figure 3 indicates the X-ray diffraction patterns and the temperature dependency of the intensity of the maximum at $\lambda = 1.54$ Å for the undecyl homologue of I. The intensity at the maximal position rapidly increases around the S_1–S_2 transition point and stays almost constant throughout the smectic A and cholesteric phases. The characteristic feature is that the maximal peak is slightly broad. Thereby, we observed a strong peak at 8.0 Å, perhaps corresponding to the molecular distance. From Figure 3A, the layer spacing was evaluated to be 43.7 Å.

Discussion

In Table V, the thermal properties of the present series are compared with those of the following homologous series selected for a comparative study. One might expect that the bend angle of 58–74° for these aryl cores would decrease the Ch–I transition temperature as well as the enthalpy and entropy.[6] Indeed, the angular effect is distinctly recognized in the Ch–I transition temperature; i.e., $T_{Ch\text{-}I}$ for both C_0 and C_{11} homologues of I–IV are lower than those of V and VI having the linear core, and $T_{Ch\text{-}I}$ for the C_{11} homologues of III and IV are slightly lower compared with those for VII having no polar core. $T_{S_A\text{-Ch}}$ for the C_{11} homologues of I and II are also lower than those for V and VI.

TABLE VI[a]

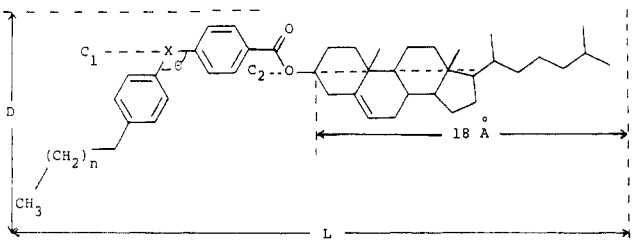

n	X	θ, deg	L, Å	D, Å	L/D	$T_{Ch\text{-}I}$, °C
0	CO	122[b]	31	9.2	3.4	210.3
1	CO	122	31	11	3.0	205.9
7	CO	122	38	13	2.8	152.8
11	CO	122	43	15	2.8	141.4
15	CO	122	48	17	2.7	127.3
11	O	118[c]	42	16	2.6	123.2
11	S	106[c]	40	19	2.1	[35]
11	CH_2	111[d]	41	18	2.3	[50]

[a] To simplify the geometry, the following items are supposed: (1) All atoms belonging to the carboxyl portion are on the plane, and the carbon atoms of the alkyl chain take a zig-zag conformation. (2) The cholesteryl portion is arranged on the same plane as the carboxy portion by neglecting the conformation aroung the ester linkage. The geometry of the cholesterol was referred to the literature. (3) The axes, C_1, for the carboxy portion and C_2 for the steroid one are parallel to each other. (4) The bond length is 1.54 Å for C–C and 1.1 Å for C–H, and the van der Waals radius is 1.0 Å for hydrogen. [b] Reference 8. [c] H. T. Peterson and D. E. Martire, *J. Chem. Phys.*, 61, 3547 (1974). [d] F. K. Fong, *J. Chem. Phys.*, 40, 132 (1964).

(6) For example, M. J. S. Dewar and R. M. Riddle, *J. Am. Chem. Soc.*, 97, 6658 (1975).

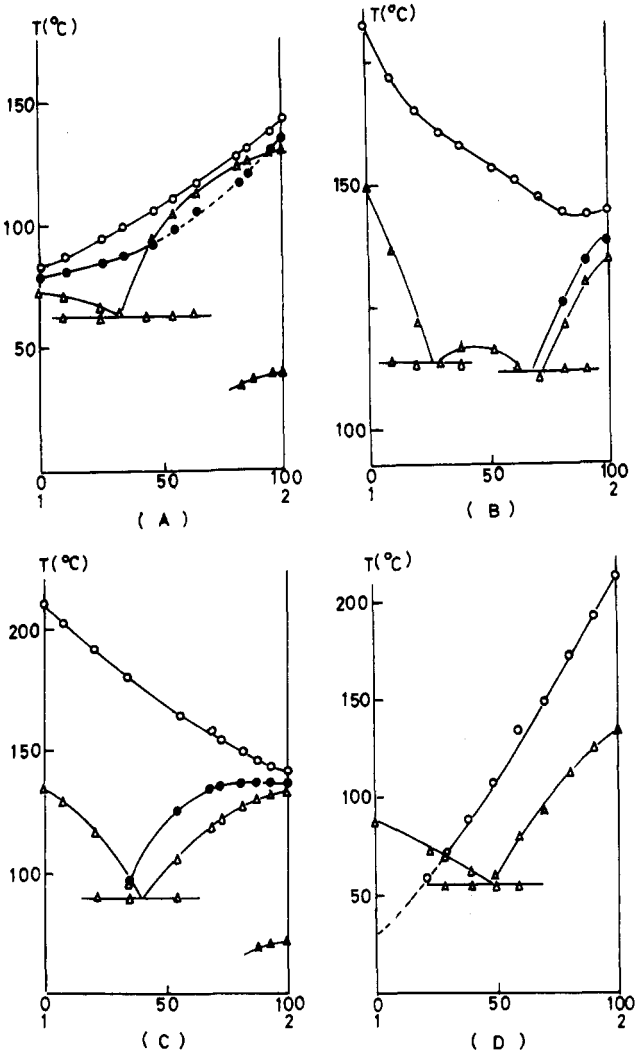

Figure 2. Isobaric diagrams of binary mixtures: A: (1) cholesteryl myristate, (2) cholesteryl 4-(4-undecylbenzoyl)benzoate. B: (1) cholesteryl benzoate, (2) cholesteryl 4-(4-undecylbenzoyl)benzoate. C: (1) cholesteryl 4-benzoylbenzoate, (2) cholesteryl 4-(4-undecylbenzoyl)-benzoate. D: (1) cholesteryl 4-[(4-undecylphenyl)thio]benzoate, (2) cholesteryl 4-benzoylbenzoate. O: Cholesteric–isotropic. ●: Smectic A–cholesteric. △: Solid–smectic A or cholesteric. ▲: Solid–solid.

We roughly estimated the molecular geometries of series I–IV based on the X-ray data,[7,8] and the results are shown in Table VI. As is evident from the table, the chain elongation leads to an increase in not only the molecular length but also the breadth. Furthermore, unlike the trend for the usual thermotropic liquid crystalline materials, the ratio of the molecular length L to the breadth D becomes small with increasing n. We have to keep in mind here that a long chain usually has some degree of flexibility and therefore the practical chain length should be different from the values in the table.[9] The cholesteric–isotropic transition temperatures for series I are plotted against the calculated L/D Figure 4. Although the trend of the cholesteric–isotropic transition temperature in Figure 1 looks rather normal,[10] it is very clear that the Ch–I transition temperature declines rapidly in Figure 4. That is, T_{Ch-I} decreases by ca. 80 °C when n increases from unity to 15, while L/D varies only 0.3, i.e., from 3.0 to 2.7. Therefore, we can conclude that the depression in the transition temperature in series I is quite large compared with those of V and VI. Usually, an introduction of substituent such as an alkyl or an alkoxy group at the terminal position has been known to increase the thermal stability of the mesophase, for it increases the molecular length and also increases the anisotropic polarity and polarizability.[1] However, the introduction of the alkyl group at the terminal position in I depresses the transition temperature. Considering the fact that the diameter of benzophenone is almost comparable with that of the cholesteryl portion, the substitution of the alkyl group at the 4′ position will result in a rapid increase in the molecular breadth, though L/D stays constant. Conclusively, the increase in the molecular breadth with increasing n is solely responsible for the rapid depression of the mesophase stability.

From a geometrical point of view, the C_0 homologue of I seems to be not so favorable for the stability of the cholesteric phase, since the L/D ratio is relatively small (3.4).[11] Nevertheless, T_{Ch-I} is higher by 150 °C than that of the C_0 homologue of VII, indicating that the anisotropic polarity and polarizability of the aryl moieties play an important role for the stability of the cholesteric phase. The effective order for the mesophase stability, CO > O > S > CH_2, also suggests the importance. Such attractive dispersion forces and/or dipole–dipole interactions would be expected to decrease progressively with increasing molecular breadth, and the infinitely increasing tendency of the molecular breadth leads to infinite reduction of the attractive dispersion forces, depressing T_{Ch-I} progressively, for example, along the dotted line in Figure 1A. Nevertheless, the homologous series onward (n = 7–15) also form stable cholesteric and smetctic A phases, and that the electronic effect of the aryl cores enough reflects on the Ch–I transition temperature. Moreover, the enthalpy and the entropy for Ch–I and Ch–S_A transitions stay constant throughout the series. These facts indicate that in the homologues with n = 7–15, the molecular distance and the intermolecular organization in the mesophases are almost unaffected by chain elongation. Accordingly, the molecular organization in the cholesteric phase and also smectic A in the heptyl to pentadecyl homologues might be slightly different from that in the earlier homologues. A characteristic feature in the later homologues is that the cholesteric phase always accompanies the smectic A phase or the solid S_2 phase just below the phase, and the cholesteric range is quite narrow (10–2 °C) and almost constant. It has been known that the cholesteric (nematic) phase just above the smectic A phase makes a large contribution to the cybotactic group of the smectic A where the molecules have a translational ordering, through the usual cholesteric phase has only orientational ordering.[12,13] Therefore, the molecular organization in the cholesteric phase is assumed to be similar to that in the smectic A phase. In the present case, a large contribution of the cybotactic group might be the cause of the appearance and enhancement of the stability of the cholesteric phase. The evidence is that the intensity of the X-ray diffraction peak arising from the layer spacing for the C_{11} homologue of I is almost constant

(7) J. H. Wendorff and F. P. Price, *Mol. Cryst. Liq. Cryst.*, **25**, 71 (1974).
(8) E. B. Fleischer, N. Sung, and S. Hawkinson, *J. Phys. Chem.*, **72**, 431 (1968).
(9) J. H. Wendorff and F. P. Price, *Mol. Cryst. Liq. Cryst.*, **24**, 129 (1973).
(10) W. Elser, J. L. W. Pohlmann, and P. R. Boyd, *Mol. Cryst. Liq. Cryst.*, **11**, 279 (1971); **20**, 87 (1973); J. S. Dave and R. A. Vora, *ibid.*, **14**, 319 (1971); J. S. Dave and G. Kurian, *ibid.*, **24**, 347 (1973).
(11) H. Kimura, *J. Phys. Soc. Jpn.*, **36**, 1280 (1974).
(12) A. De Vries, *Mol. Cryst. Liq. Cryst.*, **10**, 219 (1970); H. Arnord, *Z. Chem.*, **4**, 211 (1964); J. van der Veen, W. H. de Jeu, M. W. M. Wanninkhot, and C. A. M. Tienhoven, *J. Phys. Chem.*, **77**, 2153 (1973).
(13) W. L. McMillan, *Phys. Rev. A*, **4**, 1238 (1971).

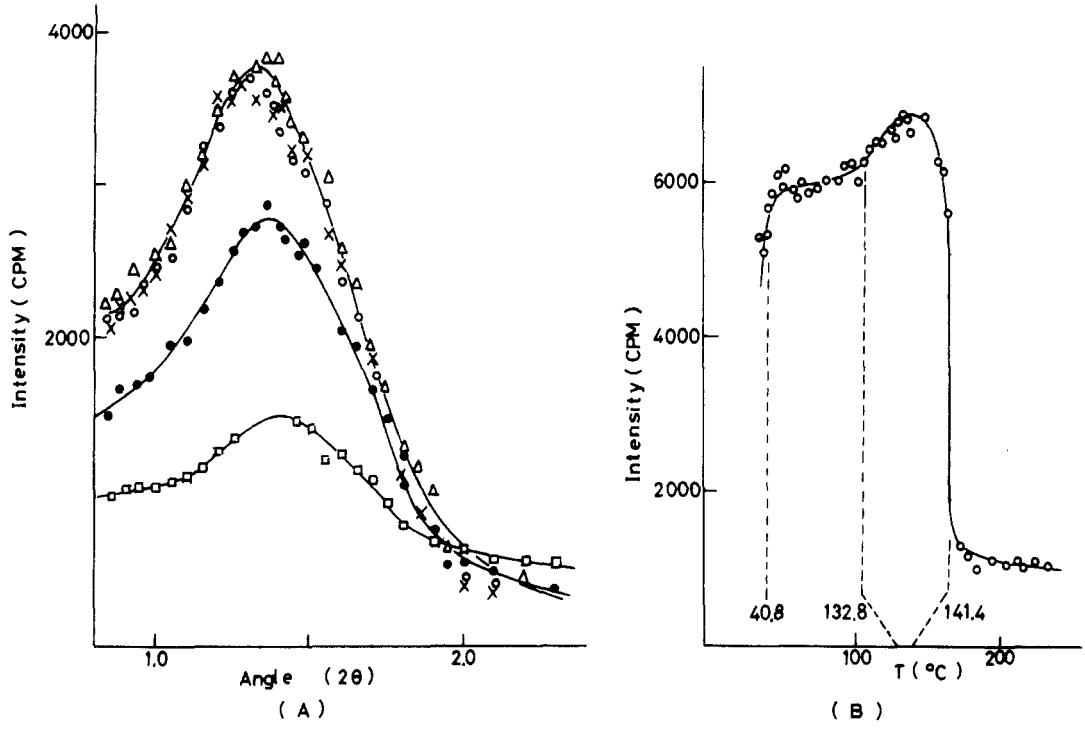

Figure 3. A: Measured X-ray scattered intensity per unit solid angle vs. scattering angle for the C_{11} homologue of I at (●) room tempeature and at (△) 87.0, (×) 134.3, (○) 138.3, and (□) 167.0 °C. B: Measured X-ray scattered intensity vs. temperature at the Bragg angle for the C_{11} homologue of I.

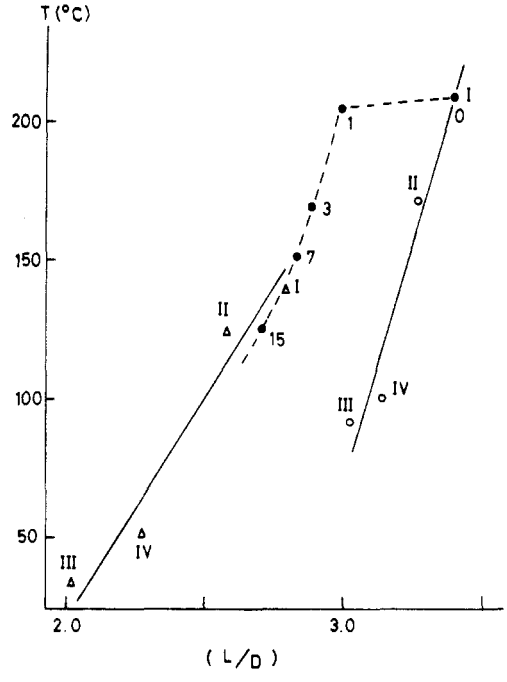

Figure 4. Plot of the cholesteric–isotropic transition temperature against the calculated L/D for (●) the homologous series of I, where the number represents the carbon number, n, (○) the C_0 homologues of I–IV, and (△) the C_{11} homologues of I–IV.

throughout the S_2, smectic A, and cholesteric phases, as shown in Figure 3B.

The role of the steroid portion in the present series seems to be especially important in determining the mesomorphic properties. As is evident from Table III, the thermal properties even for the C_{11} homologues are strongly sensitive to a subtle change in the alkyl group at the C-17 position. Therefore, one can assume that the steroid portions are closely piled up to each other in the mesophases, and the lateral interaction around the steroid portions determines the thermal properties for the present series. A remarkable trend for the present series is that the transition enthalpies and entropies for the smectic A–cholesteric and cholesteric–isotropic transitions are almost independent of the carbon number in the alkyl chain, as shown in Figure 1B. This fact indicates that the alkyl groups are slightly apart from each other in the mesophases, and have no short-range interaction which is observed in the usual thermotropic mesogens. However, considering the fact that the commencement of the smectic A phase in I and II is the same as those of series V–VII, the alkyl chain is assumed to increase the molecular distance along the longitudinal direction, and facilitate the formation of the layer organization of molecules, as well as the alkyl chain in the usual thermotropic mesogens.

Apart from the mesomorphic phenomena, there are some interesting trends in the thermal properties of the solid phases shown in Figure 1, where two crystalline states are conventionally classified into S_1 and S_2, though the identification of these phases has not been done. The rapidly decreasing trend on moving from the propionate to decanoate homologues suggests that the increase in the cylindrical diameter weakens the lattice energy of the S_1 phase. On the other hand, the incline trends of the transition temperature and entropy indicate that the short-range interactions of the alkyl chain lead to an increase in the lattice energy.

We have assumed the S_2 phase to be one of the solid phases, for it forms eutectic mixtures with the solid phases of some cholesteryl esters, as shown in Figure 2A–C. The fact that the S_2–cholesteric or –smectic A transitions release 50–90% of the total entropy also indicates that the S_2 phase is a hard phase, whereas the trend of the X-ray diffraction in Figure 3B is quite similar to that of the smectic phase. Usually, an increase in the diffractive intensity implies the formation of a layer, i.e., the formation of a smectic phase. Further investigation is now under way.

Acknowledgment. We express our thanks to Dr. H. Terauchi, professor at Kuwansei-Gakuin University, for

the X-ray measurements and many helpful discussions.

Registry No. I (n = 0), 74997-33-4; I (n = 1), 77069-42-2; I (n = 2), 77069-43-3; I (n = 3), 77069-44-4; I (n = 4), 77069-45-5; I (n = 5), 77069-46-6; I (n = 6), 77069-47-7; I (n = 7), 77069-48-8; I (n = 8), 77069-49-9; I (n = 9), 77069-50-2; I (n = 10), 77069-51-3; I (n = 11), 77069-52-4; I (n = 13), 77069-53-5; I (n = 15), 77069-54-6; II (n = 0), 74997-31-2; II (n = 6), 87100-37-6; II (n = 9), 87100-38-7; II (n = 10), 87100-39-8; II (n = 11), 87100-45-6; III (n = 0), 74997-32-3; III (n = 9), 87100-40-1; III (n = 10), 87100-41-2; III (n = 11), 87100-42-3; IV (n = 0), 83038-71-5; IV (n = 10), 87100-43-4; IV (n = 11), 87100-44-5; $C_{11}H_{23}$-p-C_6H_4-CO-p-C_6H_4-COOR (R = cholestanyl), 87100-46-7; $C_{11}H_{23}$-p-C_6H_4-CO-p-C_6H_4-COOR (R = β-sitosteryl), 87100-47-8; $C_{11}H_{23}$-p-C_6H_4-CO-p-C_6H_4-COOR (R = stigmasteryl), 87100-35-4; $C_{11}H_{23}$-p-C_6H_4-CO-p-C_6H_4-COOR (R = ergosteryl), 87100-36-5; cholesteryl myristate, 1989-52-2; cholesteryl benzoate, 604-32-0; cholesteryl 4-benzoylbenzoate, 74997-33-4.

Oil-in-Water Microemulsion Globules as Carriers of Lipophilic Substances across Liquid Membranes

A. Xenakis and C. Tondre*

Laboratoire de Chimie Physique Organique, E.R.A. C.N.R.S.222, Université de Nancy I, B.P. 239, 54506 Vandoeuvre-les-Nancy Cedex, France *(Received: November 17, 1982; In Final Form: March 28, 1983)*

The carrier properties of microemulsion droplets were investigated by using biphasic systems of the Winsor I type (that is, constituted of an oil phase floating on the top of an oil-in-water (o/w) microemulsion phase). The systems investigated were constituted of sodium dodecyl sulfate (SDS)/1-pentanol/n-dodecane/water (or brine). The microemulsion was used as a liquid membrane between two oil phases (a "source" phase and a "receiving" phase) and the rate of transfer of neutral arenes (pyrene, perylene, and anthracene), practically insoluble in the water continuous phase of the microemulsion, was determined from UV spectrophotometric measurements. The influence of different parameters on the transported solutes was studied: initial concentration of solute in the source phase, composition of the microemulsion, salt concentration. The results are shown to be consistent with a model in which the diffusion of droplets is coupled with a fast solubilization–desolubilization process and other possible mechanisms are critically examined. Some information is obtained concerning the thermodynamics of solubilization–desolubilization of neutral arenes in microemulsion droplets. The results also allow one to get an insight into the structural organization of the microemulsion investigated: when the oil content of the microemulsion phase becomes higher than 12% in weight, a dramatic increase of the transfer rate of solute is observed which has been attributed to the percolation of oil droplets preceding the formation of bicontinuous phases.

Introduction

The tremendously increasing interest which is developing in the literature concerning microemulsion systems arises essentially from their numerous potential applications in various branches of modern science or technology. As examples, the use of microemulsions in the following fields can be mentioned: tertiary oil recovery,[1] chemical energy production from water cleavage,[2] metal recovering from liquid–liquid extraction,[3] development of potential blood substitutes[4] (this list is far from exhaustive).

Among these applications are those related to the possibility of using such systems to carry lipophilic substances through an aqueous medium or inversely to carry hydrophilic substances across a lipoidic medium. We have recently given a short preliminary report[5] on results concerning this aspect of the physical chemical properties of microemulsions which had not received much attention so far. In this paper we intend to investigate in more detail the kinetics of the transport of lipophilic substances (neutral arenes) by oil-in-water microemulsion globules and the mechanism involved in this process.

The method used was mainly suggested to us by the numerous studies dealing with the transport of metal ions across liquid membranes, using antibiotics or macrocyclic carriers,[6-9] but a number of experimental difficulties had to be overcome before successful experiments could be performed.

The results obtained have some implications regarding the thermodynamics of solubilization–desolubilization of neutral arene in (outside of) a microemulsion droplet and they are, as expected, very much dependent on the structural organization of the system investigated.

Experimental Section

Chemicals. The origins of the chemicals used were the following: n-dodecane, 1-pentanol, pyrene, perylene, anthracene from Fluka (purum or puriss); sodium dodecyl sulfate (SDS) from Serva (Heidelberg, W.G.). All these chemicals were used as supplied.

Preparation and Characterization of Biphasic Systems. The biphasic systems used in this study were obtained from compositions chosen in the pseudoternary diagram represented in Figure 1, where the components are SDS/1-pentanol/n-dodecane/H_2O. The weight ratio be-

(1) V. K. Bansal and D. O. Shah in "Micellization, Solubilization and Microemulsions", Vol. 1, K. L. Mittal, Ed., Plenum Press, New York, 1977.
(2) J. Kiwi and M. Grätzel, *J. Am. Chem. Soc.*, **100**, 6314 (1978).
(3) P. Fourre and D. Bauer, *C. R. Hebd. Seances Acad. Sci., Ser. B*, **292**, 1077 (1981).
(4) G. Mathis and J.-J. Delpuech, French Patent 8022875, 1980; G. Mathis, D.Sc. Thesis, University of Nancy I, Nancy, France, 1982.
(5) C. Tondre and A. Xenakis, *Colloid Polym. Sci.*, **260**, 232 (1982).
(6) R. Ashton and L. K. Steinrauf, *J. Mol. Biol.*, **49**, 547 (1970).
(7) K. H. Wong, K. Yagi, and J. Smid, *J. Membr. Biol.*, **18**, 379 (1974).
(8) C. F. Reusch and E. L. Cussler, *AIChE J.*, **19**, 736 (1973).
(9) J. D. Lamb, J. J. Christensen, S. R. Izatt, K. Bedke, M. S. Astin, and R. M. Izatt, *J. Am. Chem. Soc.* **102**, 3399 (1980).

0022-3654/83/2087-4737$01.50/0